Am J Cancer Res 2021;11(2):441-457
www.ajcr.us /ISSN:2156-6976/ajcr0126519

Original Article

Isolation and characterization of cancer stem cells derived from human glioblastoma

Hiroko Ishii[1], Yuki Mimura[2], Maram H Zahra[2], Shota Katayama[2], Ghmkin Hassan[2], Said M Afify[2,3], Masaharu Seno[2]

[1]GSP Enterprise, Inc., 1-4-38 12F Minato-machi, Naniwaku, Osaka 556-0017, Japan; [2]Laboratory of Nano-Biotechnology, Graduate School of Interdisciplinary Science and Engineering in Health Systems, Okayama University, Okayama 700-8530, Japan; [3]Division of Biochemistry, Chemistry Department, Faculty of Science, Menoufia University, Shebin ElKoum Menoufia, 32511, Egypt

Received November 18, 2020; Accepted December 15, 2020; Epub February 1, 2021; Published February 15, 2021

Abstract: Cancer stem cell (CSC) is considered as a cause of cancer recurrence and metastasis. Simultaneously CSCs are responsible for the heterogeneous population in tumor tissues due to their differentiation potential. However, the characterizations of CSCs are still not enough and cancer stem cell lines widely available is desired to be established for the advancement of cancer research. In this study, we tried to isolate and characterize stem like cells from human glioblastoma cell line U-251MG cells. U-251MG P1 cells, which was previously condensed in the presence of hyaluronic acid as CD44 positive population were subjected to single cell isolation procedure. Although 5 clones were isolated, only one clone exhibited high expression of CD44, Nanog, OCT3/4 and SOX2, and named U-251MGSC1. The sphere forming ability of U-251MGSC1 cell was significantly higher than the parental U-251MG cells. Tumorigenicity of U-251MG-SC1 cells were higher than that of U-251MG cells. U-251MGSC1 cells exhibited higher expression of CD44, SOX2, Nestin and A2B5 than U-251MG cells in vitro and in vivo. The expression of GFAP and NF-M was enhanced when the cells were treated with the conditioned medium of U-251MG cells indicating the potential of differentiation. Sphere forming ability was more efficient than that of U-251MG cells and was enhanced in the presence of hyaluronic acid, which enhanced the cell growth as well. U-251MGSC1 cells exhibited rapid growth tumor in nude mice and efficient metastatic ability in transmembrane assay when compared with U-251MG cells. As the result, we concluded U-251MGSC1 cell was a glioblastoma CSC line derived from the parental U-251MG cells. U-251MGSC1 cells will be a good tool to develop effective therapeutic agents against CSCs and to elucidate the properties of glioma derived CSCs and the mechanism of tumor development in brain.

Keywords: Cancer stem cell, glioblastoma, sphere formation, CD44, SOX2, GFAP

Introduction

Studies in 2019 has shown that cancer became the number one cause of death in advanced countries [1]. Current development of cancer treatment is highly competitive and new therapeutic agents and treatments are commercialized around the world. Surgical operation, chemo- and radiation-therapy are mainly used for cancer treatment (**Table 1**). However, it is sometimes extremely difficult to eliminate tumor cells completely resulting in the growth of residual cells and the recurrence. CSC is emphasized due to its cells resistant to chemotherapy and radiation surviving as a cause of recurrence and metastasis and many studies have proved its system [2, 3]. CSCs have been shown pluripotent, self-renewing and able to form tumors similar to the original one even from a small number of cells [4, 5]. Therefore, some researchers consider CSCs should be the potential target of treatment against cancer including recurrence and metastasis characterizing CSCs in more details [6-8]. However, it is still difficult to establish CSC lines since the procedures to isolate CSCs from cancer cell lines or cancer tissues have not been well established. Generally, cell lines contain heterogeneous population of cells. Many cell lines are described to be isolated as subclones from their parental cells. For instance, NTER2 D1 cells [9, 10] are the

Table 1. Features of each cancer treatment method

Therapeutic methods		Advantage	disadvantage	CSC targetability	ref
Chemotherapy	Anti-cancer agent	■ Therapeutic effect on systemic cancer	■ Severe side effects		
	■ Paclitaxel		■ Induction of chemoresistance	NS*1	[58]
	■ Cisplatin			NS	[59]
	■ Doxorubicin			NS	[60]
	Anti-Cancer stem cell	■ Disperse side effects	■ Changes in normal stem cells to CSC		
	■ Metformin (Type 2 anti-diabetic)	■ Less chance of developing chemoresistance	■ Induction of toxicity to normal tissues and organs	S*2	[61]
	■ Mithramycin (RNA synthesis inhibitor)	■ Very effective against cancer metastasis and recurrence	■ Potential increased risk of drug resistance	S	[61]
		■ Expected to cure cancer			
	Combination	■ Antigen specific	■ Large cost burden		
	■ Opdivo/Yervoy	■ Disperse side effects	■ Strict attention to dosage and frequency of administration	NS	[62]
	■ Gefitinib/Carboplatin/Pemetrexed	■ Reduces the chance of developing treatment-resistant cancer cells		NS	[63]
	■ Vismodegib (Hedgehog inhibitor)/Gemcitabine			S	[61]
	DDS	■ Reduces side effects	■ Difficulty in technological development		
	■ Trastuzumab-monomethyl auristatin E conjugate	■ Improves therapeutic effect	■ Long development period and high cost	NS	[64]
	■ Brentuximab Vedotin			NS	[65]
	■ Doxil			NS	[66]
	■ Irinotecan liposomes (Onyvyde)			NS	[67]
Radiation	■ Gamma knife	■ Less physical burden	■ Side effects due to the irradiation site	NS	
	■ Heavy ion beams	■ Painless			
	■ BNCT				
Surgery	■ Resection	■ Complete cure by cancer tissue resection	■ Heavy burden on the body	NS	
	■ Laparotomy		■ Ineffective for recurrence and metastatic cancer		
	■ Laparoscopic surgery				

*1: Non-specific. *2: Specific.

subclone of human teratocarcinoma cell line NTERA-2 cells [11], which are the subclone of human teratocarcinoma cell line Tera-2 [12]. Also MCF10A and MCF10F cells were subcloned from human breast epithelial cell line MCF-10 cells [13]. This is conceivable if the cell lines contain stem cell population, which makes heterogeneity as the results of differentiation.

We have been aiming to discover new therapeutic targets that are closely associated with recurrence and metastasis. During the course of time, we have come across with CSCs, which are important in the recurrence and metastasis. However, the difficulty to obtain CSCs has been a substantial problem to make the progress as found in many cases of CSC studies. Therefore, we started to establish CSC lines to discover the drug targets that are specific to CSCs. The first target we focused on was glioma, which has a high recurrence rate and is difficult to treat. Typical brain tumors include glioma, meningioma, schwannoma, and pituitary adenoma, some of which can be cured by surgical removal, but most are surgically removed with additional drug or radiation therapy. Astrocytoma in the category of glioma accounts for approximately 20% of brain tumors. Originating from astrocytes, which is the main constituent cells of the brain, astrocytoma is a malignant tumor in almost all cases with a strong character to infiltrate the surrounding brain tissue. As the result, only surgical resection following craniotomy is not sufficient to remove astrocytoma completely [14]. Such a highly malignant glioma is generally treated with the combination of surgery, chemotherapy, and radiation therapy. However, glioma mortality and recurrence rates are very high and patient survival is very poor [15]. The prevention and the development of effective treatments of glioma are under investigation and the etiology is still unknown.

In this study, we tried to isolate and establish CSC lines from human glioma cell line U251MG P1 cells using hyaluronic acid because we have already identified the overexpression of CD44 in this cell line [16]. Since CD44 is well known as a CSC marker, here we describe the procedure is efficient to isolate CSCs with the self-renewal, differentiation and tumorigenic potential.

Materials and methods

Cell culture

Human brain glioblastoma cell line U-251MG [17, 18] was obtained from ATCC (VA). U-251MG and U-251MG P1 cells were maintained in DMEM with high glucose formula (Wako, Japan) containing 10% FBS (Thermo Fisher Scientific, MA) and 1% Penicillin-Streptomycin (nacalai tesque, Kyoto, Japan) under the atmosphere of 5% CO_2 at 37°C. The effect of 100 μg/mL hyaluronic acid sodium salt (Wako, Japan) on the growth of the cells were assessed in DMEM with high glucose formula containing 10% FBS and 1% Penicillin-Streptomycin at 37°C under the atmosphere of 5% CO_2. The culture medium was replaced every 2 days.

Single cell cloning

U-251MG P1 cells were suspended in high glucose DMEM containing hyaluronic acid and seeded at 1.0×10^4 cells/mL into a 60-mm culture dish (Ultra low attachment, Corning, NY) and cultured under the atmosphere of 5% CO_2 at 37°C for 10 days to form spheres. These spheres were centrifuged at 800 rpm for 3 min at 20°C and cultured in high glucose DMEM with 10% FBS and 1% Penicillin-Streptomycin at 37°C under 5% CO_2. After 3 days, cells were seeded into 10 96-well plates at 0.5 cells/well. Cells grew in each well were detached with 50 μL of 0.025% trypsin and the reaction was stopped by adding 150 μL of culture medium. After the cells were centrifuged and cells were suspended in 1 mL of culture medium. Then the cells were seeded into a well in 24-well plate (TPP, Switzerland) and cultured under 5% CO_2 at 37°C. According to the cell growth cells, the sizes of the dishes were scaled up to 12-well plate, 6-well plate, 60-mm dish, and 100-mm dish (TPP, Switzerland).

Real time PCR

Approximately 1.0×10^6 cells were homogenized in 1 mL of TRIzol® Reagent (Thermo Fisher Scientific, MA). After addition of 200 μL of chloroform (FUJIFILM, Japan), the solution was vortexed for 2 min and then incubated for 2 min at 25°C. After centrifugation at 12,500 g for 15 min at 4°C, the supernatant was transferred to another 1.5 mL-tube. To remove the residual phenol 700 μL of chloroform was

Table 2. The list of primers used for rt-qPCR

Target gene name	GenBank accession	Foward primer (5'→ 3')	Reverse primer (5'→ 3')
GAPDH	NM_001357943.2	CAACGACCACTTTGTCAAGCTC	GGTCTACATGGCAACTGTGAGG
SOX2	NM_003106.4	GGGAAATGGGAGGGGTGCAAAAGAGG	TTGCGTGAGTGTGGATGGGGATTGGTG
c-MYC	NM_002467.6	GCGTCCTGGGAAGGGAGATCCGGAGC	TTGAGGGGCATCGTCGCGGGAGGCTG
OCT3/4	NM_002701.6	GACAGGGGGAGGGGAGGAGGTAGG	CTTCCCTCCAACCAGTTGCCCCAAAC
KLF4	NM_001314052.2	ATGCTCACCCCACCTTCTTC	TTCTCACCTGTGTGGGTTCG
Nanog	NM_024865.3	ACCTCAGCTACAAACAGGTGAA	AAAGGCTGGGGTAGGTAGGT
Olig2	NM_005806.4	CCGATGACCTTTTTCTGCC	ATGACTTGAAGCCACTGCC
CD44	NM_000610.3	TGGGTTCATAGAAGGGCACG	AGGTGGAGCTGAAGCATTGAA
Nodal	NM_018055.5	AGACATCATCCGCAGCCTACA	GACCTGGGACAAAGTGACAGTGAA
Nestin	NM_006617.2	ATGCTCCTCTCTCTCTGCTC	TTCTTTCTCTACCAACCCCC

Table 3. Tm values employed for rt-qPCR

Target gene name	Tm value	Target gene name	Tm value
GAPDH	57	Nanog	63
SOX2	57	CD44	57
c-MYC	60	Nodal	54
OCT3/4	60	Nestin	54
KLF4	57	Olig2	57

added and centrifuged. The resultant supernatant was mixed with 250 μL of isopropanol (Sigma Aldrich, MO) and left standing at 25°C for 10 min to precipitate nucleic acid. After centrifugation at 12,500 g for 10 min at 4°C, the precipitate was dissolved in 100 μL of DEPC-treated water. After adding 10 μL 3 M sodium acetate (nacalai tesque, Japan) the nucleic acid was precipitated again with 250 μL of ethanol (FUJIFILM, Japan) by the incubation at -20°C. After centrifuged at 16,000 g for 10 min at 4°C the pellet was rinsed with 500 μL of 75% ethanol. After centrifugation at 7,500 g for 5 min at 4°C, the supernatant was disposed and the pellet was air dried. The pellet was completely dissolved in 30 μL of DEPC-treated water by incubation at 60°C for 10 min (Cool Thermo Unit CTU-Neo, TAITEC, Japan) and then the concentration of nucleic acid was measured by NANO VUE (GE Healthcare Japan).

To remove DNA, 3 μg of nucleic acid was treated with 2 units of DNase I (1 unit/μL, Promega, WI) in 20 μL of reaction volume at 37°C for 30 min. The reaction was stopped with 2.5 μL of 25 mM EDTA followed by the incubation at 65°C for 10 min and the residual RNA was precipitated with ethanol and resolved in 30 μL of DEPC-treated water.

To 2 μg of RNA, 1 μL of 50 μM oligo-dT was added and the mixture was incubated at 70°C for 5 min and chilled on ice. Then cDNA was synthesized with the GoScript™ Reverse Transcription System (Promega, WI).

PCR was performed to amplify each target gene in a 96-well plate (Light Cycler 480 Multiwell Plate, Roche). The primers employed in this study are summarized in **Tables 2** and **3**. Each reaction was composed of 0.8 μL each of forward and reverse primers in 10 μM, 10 μL of GeneAce SYBER qPCR Mix alpha No ROX (NipponGene, Japan) and 6.4 μL of milli-Q water and 2 μL of the cDNA solution. Light Cycler 480 (Roche, Switzerland) was used for the real time measurement. The conditions of reaction are enzyme activation at 95°C for 10 min flowed by 45 cycles of denaturing at 95°C for 30 sec and polymerase reaction at 60°C for 1 min.

Flow cytometry

U251MG cells, U251MG P1 cells and U251MG-SC1 cells confluent in 60-mm dishes were washed with PBS twice and the cells were detached with 0.0025% trypsin. After suspended in 100 μL of PBS containing 10% FBS, cells were mixed with 1 μL of Pharmingen™ APC Mouse Anti-Human CD44 (Becton, Dickinson and Company, NJ, 2292642) and 1 μL of PE anti-human CD133 (BioLegend®, CA, B262394) and incubated on ice for 30 min. The cells were then centrifuged at 800 rpm for 3 min at 25°C and washed with PBS containing 10% FBS. The cells were finally suspended in 150 μL of PBS containing 10% FBS passed through a nylon mesh. An Accuri™ C6 Plus Flow Cytometer (Becton, Dickinson and Company, NJ) was used for the measurement.

Western blotting

Ten μg of protein from each sample was applied to SDS-PAGE and electrophoretically transferred to PVDF membrane (Merck Millipore, MA). Membrane was blocked with 5% skim milk and incubated at 4°C overnight with anti-GFAP antibody (J0510, Santa Cruz Biotechnology, CA) diluted to 1/1000 or anti-β-actin antibody (4970S, Cell Signaling, MA) diluted to 1/1000. After wash with TBST for 3 times, membrane was incubated with anti-mouse IgG-HRP (sc-200s, Santa Cruz Biotechnology, CA) diluted to 1/1000 or Anti-rabbit IgG-HRP (Cell Signaling, 7074S, diluted to 1/1000). Immunoreactive bands were developed with Western Lightning™ Plus-ECL (Perkin Elmer, MA) and observed by Light Capture II system (ATTO, Tokyo, Japan).

Limiting dilution analysis

U-251MG and U-251MGSC1 cells were suspended in DMEM-High glucose (Wako, Japan) with 1% ITS-X (Fujifilm, Japan), 1% L-Glutamine (nacalai tesque, Japan), 1% NEAA (Fujifilm, Japan), 0.5% beta-mercaptoethanol (Sigma-Aldrich, MO), 1% Penicillin/Streptomycin and 100 μg/mL hyaluronic acid sodium salt (Wako, Japan). Cells were plated at 20, 10, 5, 2.5, 1.25 and 0.625 cells/well into a Prime Surface 96-V-plate (Sumitomo Bakelite, Japan). Then the cells were incubated at 37°C under the atmosphere of 5% CO_2. After 2 weeks, the number of wells, in which the sphere formation was confirmed, was counted and analyzed as previously described [19, 20].

Proliferation assay

We prepared DMEM high glucose supplemented with 10% FBS and 1% penicillin streptomycin with and without hyaluronic acid (100 μg/mL). After plating 1×10^4 U-251MG cells and U-251MGSC1 cells on a 24-well plate, the number of cells was counted every 2 days from the next day up to day 9. All cells got confluent after 11 days. Sphere formation medium with or without hyaluronic acid was prepared and the sphere forming ability was compared by the Limiting dilution assay. Two weeks after cell seeding, the number of spheres were counted. The limiting dilution analysis was graphed using ELDA software [21, 22]. It is especially suitable for analyzing limiting dilution data in stem cell research.

Differentiation assay

Approximately 30% confluent U-251MG cells were seeded on a 10-cm dish. After 4 days, the culture CM was collected and passed through a 0.2 μm filter. The CM was supplemented up to 10% or 50% in the fresh medium of U-251MGSC1 cells. Then the cells were cultured for 2 weeks with medium exchange every 2-day followed by sufficient passage before confluency at 37°C, 5% CO_2. The expression of each protein were confirmed by immunofluorescent staining. After fixing with 4% paraformaldehyde at room temperature for 20 minutes, the glass plate were washed 3 times and incubated with 0.1% Triton X-100 in PBS at room temperature for 10 minutes. After blocking with 2% BSA for 1 hr at room temperature, the cells were incubated with the primary antibodies overnight at 4°C. The information on the primary antibodies is as following. Anti-GFAP antibody (J0510, Santa Cruz Biotechnology, CA) (dilution 1:50), anti-Nestin antibody (N6413, Sigma Aldrich, MO) (dilution 1:100), anti-NF-M antibody (BML-NA1216, Enzo, NY) (dilution 1:50) and anti-A2B5 antibody (130-097-864, Miltenyi Biotec, CA) (dilution 1:50). After washing 3 times, the secondary antibody was incubated at room temperature for 1 hr. Alexa flour488 anti-mouse antibody (A11001, invitrogen, MA), Alexa flour488 anti-rabbit antibody (A21206, invitrogen, MA) and Alexa flour555 anti-rabbit antibody (A21428, invitrogen, MA) were used as secondary antibodies. Vectashield Hardset (VECTOR, CA) was used for DAPI staining.

Animal experiments

The animal experiment was reviewed and approved by the ethics for animal experiments at the Okayama University under the ID OKU-2017541. All experiments and the animal care were performed following to the policy of Okayama University. 10 nude mice (Balb/c-nu/nu, female, four weeks) were purchased from Charles River (Kanagawa, Japan). They fed with sterilized food and water during the experiments. 2×10^6 cells were injected subcutaneously in mice with 200 μL of Matrigel (Corning, USA) in PBS.

At the end of the experiments, all of the mice were euthanized by the isoflurane-euthanasia method [23]. Briefly, 5% isoflurane (DS Pharma animal health, Japan) was exposed to the mice

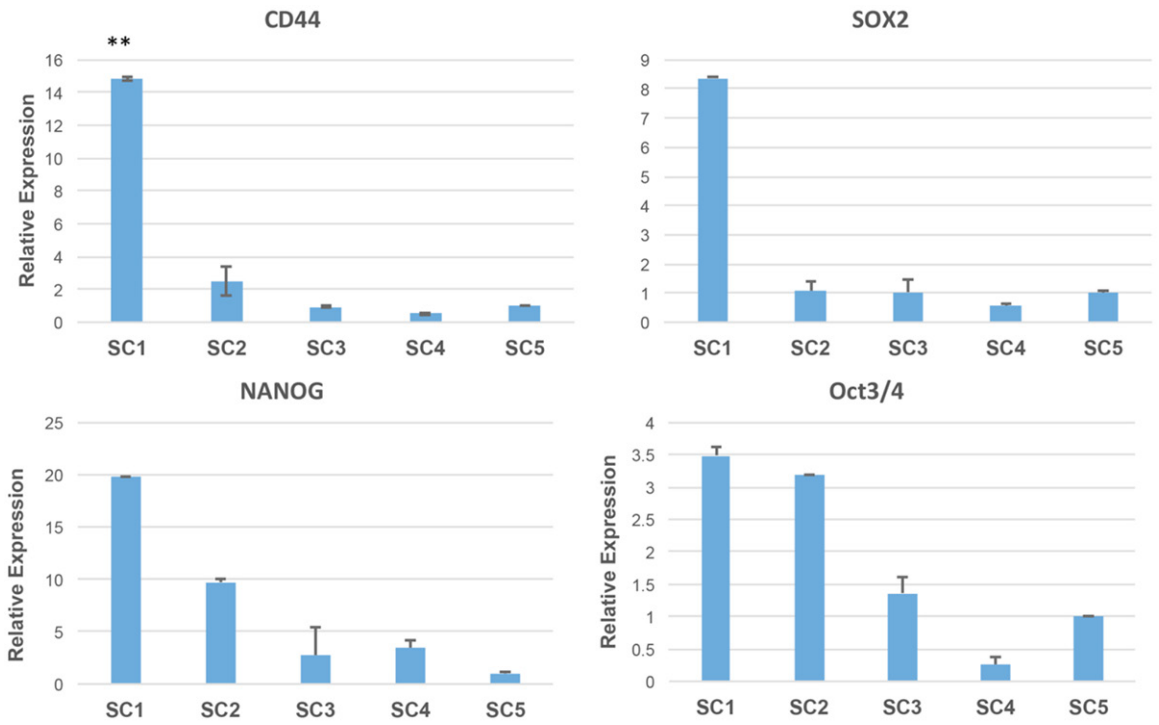

Figure 1. Comparison of stem cell marker expression in 5 cell clones by rt-PCR. SC1, SC2, SC3, SC4, SC5 cells indicate newly isolated 5 clones; U251-MGSC1, U-251MGSC2, U-251-MGSC3, U-251MGSC4, U-251MGSC5. ANOVA was employed to confirm the significant difference in each graph. n=3, *P<0.05 and **P<0.01. Relative expressions are based on SC5.

for several minutes. And euthanasia was confirmed by cervical dislocation.

Immunohistochemistry

First, 5-μm paraffin sections were boiled in 10 mM Na-Citrate, pH 6.5 for 30 min under high pressure [24, 25]. Paraffin or 5-μm frozen sections of mouse subcutaneous tumors were exposed to hydrogen peroxide for 20 min to reduce endogenous peroxidase activity. And they exposed to horse serum to block the non-specific protein binding. Then the sections were blocked with 5% skim milk, incubated with anti-CD44 antibody (ab24504, abcam, CA) diluted to 1 μg/mL, Smad2 (D43B4) XP® Rabbit mAb (3579s, Cell Signaling) diluted to 1/100 and GFAP (2A5) Antibody (Santa Cruz, sc-65343) diluted to 1/100 at 4°C overnight. After three rinses with PBS, the sections were incubated with biotinylated anti-rabbit IgG or a peroxidase anti-mouse IgG secondary antibodies (Vectastain ABC kit, Vector laboratory, CA) at 25°C for 1 hr. After three rinses in the PBS, color was developed by incubation with diaminobenzidine and H_2O_2 (Peroxidase substrate kit DAB, Vector laboratories, Inc., CA). The results of the staining were observed with a microscope FSX100 (OLYMPUS, Tokyo, Japan).

Transmembrane assay

Cells in 1.0 × 10^5 were seeded on ThinCert, 24-well, cell culture insert, TC pore diameter 8.0 μm (Greiner Bio-One International, Austria) with serum-free DMEM high medium. Then 500 μL of the DMEM high medium with 10% FBS was added in each well. The cells were kept cultured for 48 hr at 37°C under 5% CO_2. The cells, which did not transfer the membrane, were removed and the transferred cells were fixed and stained with Diff-Quik® (Sysmex Corporation, Japan).

Results

Single cell isolation

First, the spheres of U-251MG P1 cells were subjected to single cell isolation to obtain 5 cell clones, which were named as U-251MGSC1, U-251MGSC2, U-251MGSC3, U-251MGSC4, and U-251MGSC5. First, the expression CD44 gene in these cells was confirmed by RT-PCR (**Figure 1**). It has been shown

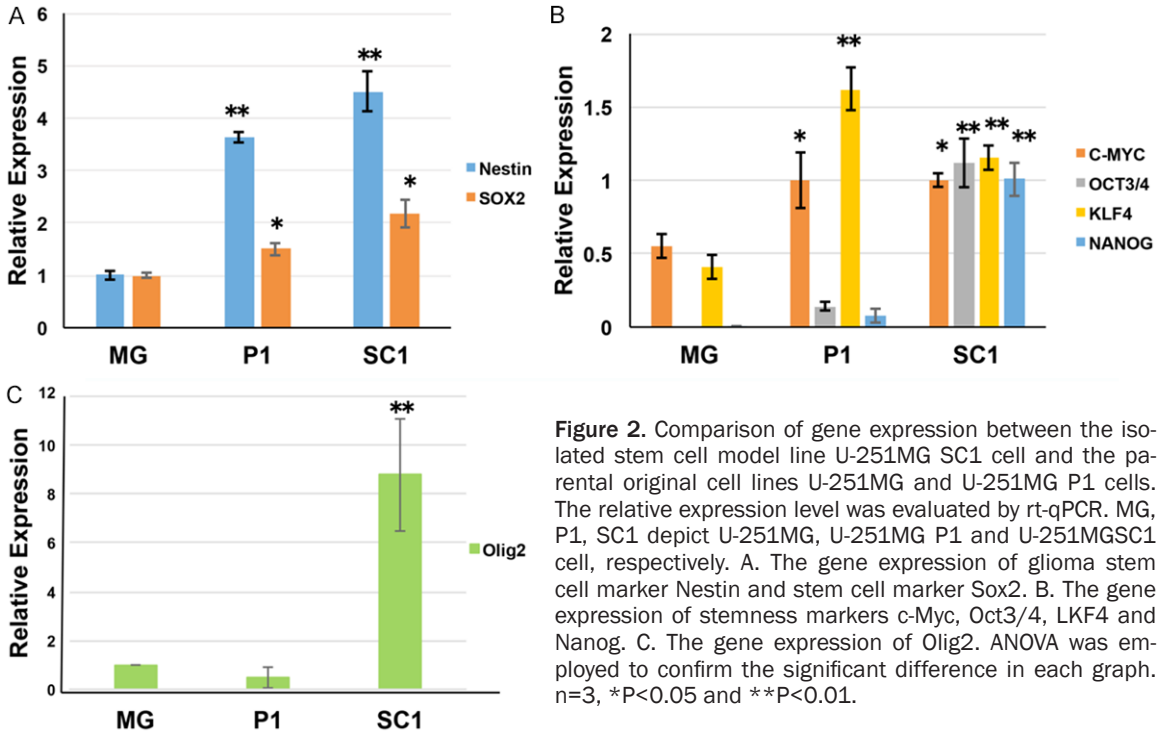

Figure 2. Comparison of gene expression between the isolated stem cell model line U-251MG SC1 cell and the parental original cell lines U-251MG and U-251MG P1 cells. The relative expression level was evaluated by rt-qPCR. MG, P1, SC1 depict U-251MG, U-251MG P1 and U-251MGSC1 cell, respectively. A. The gene expression of glioma stem cell marker Nestin and stem cell marker Sox2. B. The gene expression of stemness markers c-Myc, Oct3/4, LKF4 and Nanog. C. The gene expression of Olig2. ANOVA was employed to confirm the significant difference in each graph. n=3, *P<0.05 and **P<0.01.

that CD44 is related with the malignancy of glioblastoma [19, 26, 27]. The expression of CD44 was the highest in U-251MGSC1 cells among the other clones. Also the expression of the stemness markers such as SOX2, Nanog, and Oct3/4 genes were assessed and U-251MGSC1 cells were found to show the highest expression of these genes among the cells compared. The gene expression of the stemness markers, SOX2 [28, 29], OCT3/4 [30, 31], Nanog [32, 33], c-Myc [34-36], Olig2 [37, 38], KLF-4 [39-41] and Nestin [42] were then compared between U-251MGSC1 cells and the parental cells. As the results, the expression of the glioma stem cell marker, Nestin, and the stem cell markers, SOX2, OCT3/4 Nanog, KLF-4 and c-Myc were found the highest in U-251MGSC1 cells when compared with the parental cells (**Figure 2**). The expression of KLF-4 was observed high in U-251MG P1 and U-251MGSC1 cells when compared with the original U-251MG cells. These results indicate that U-251MGSC1 cells are found to express major stem cell markers in presumably high level when compared with the parental cells. However, the expression levels of integrin α6 and L1CAM, which were known as ones of the glioma stem cell markers, did not show much difference between U-251MGSC1 cells and the parental cells (data not shown). In the expression of L1CAM, there appears some relative difference but the expression levels were so low that we considered there was little difference in the expression level between the assessed cell lines.

Characterization of the isolated clone

Expression of CD44, CD133 and Glial fibrillary acidic protein.

U-251MGSC1 cells were further analyzed by flow cytometer comparing the markers CD44 and CD133. CD133 is a protein belonging to the prominin family, also known as PROM1 (prominin-1) or AC133. CD133 has been suggested to be a cell surface marker for adult stem cells and has also been reported as a cancer stem cell marker in various human tumors [43]. Therefore, we assessed CD44 and CD133 expression. The population of the cells with both CD44 and CD133 positive cells was the highest as 42.0% while those of U-251MG and U-251MG P1 cells were 29.2% and 26.5%, respectively (**Figure 3A**). Looking into the population of $CD44^{high}$, it was found 5.9%, 1.2% and 1.0% in U-251MGSC1, U-251MG P1 and U-251MG cells, respectively. It is worthwhile noticing that U-251MGSC1 exhibited the highest expression of CD44. Since U-251MG cells were derived from glioma, the expression of

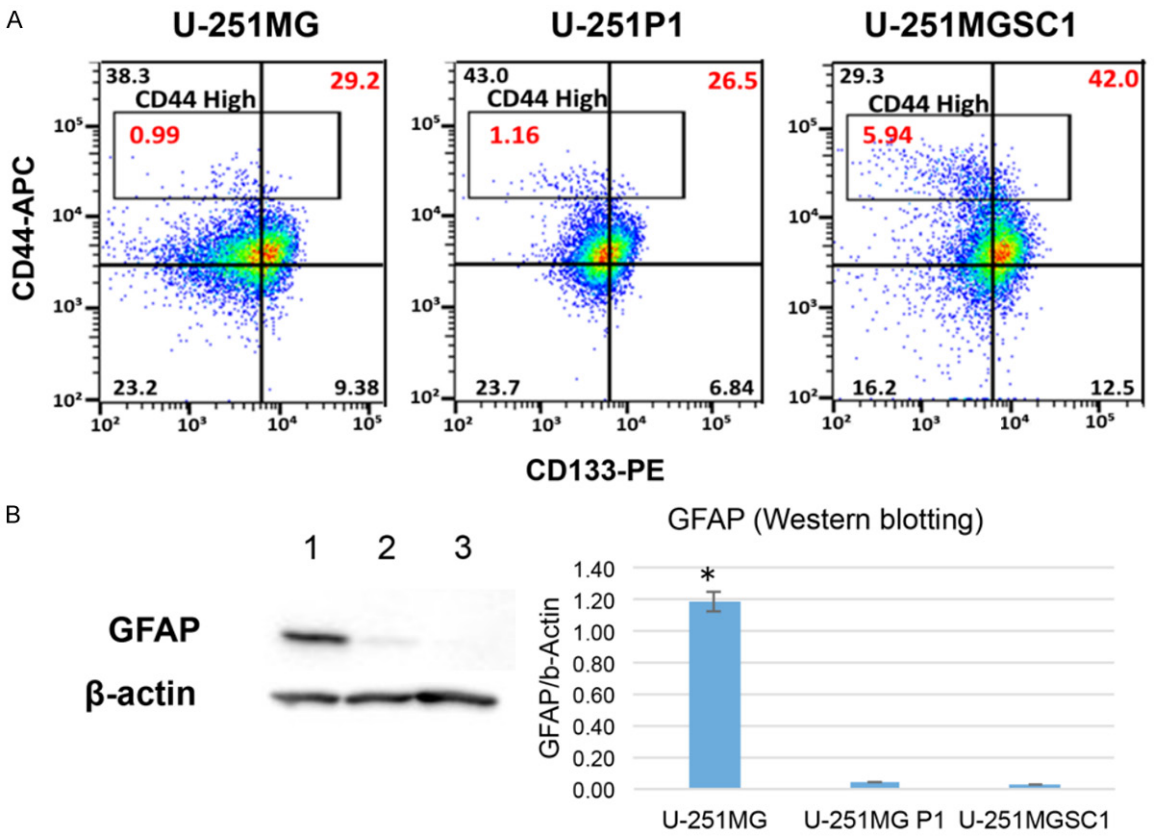

Figure 3. Expression of markers for CSC and differentiation. A. Flow cytometric analysis of for CSC markers. The vertical and horizontal axes represent CD44 and CD133, respectively. Red numbers in the top right indicate the percentage of cells positive for both CD44 and CD133. Red numbers in the boxes indicate the percentage of cells with high CD44 expression. B. Western blotting detecting GFAP as the differentiation marker of glial cell. Each lane shows extracts from U251MG cells (lane 1), U251MG P1 cells (lane 2), and U251MGSC1 cells (lane 3). ANOVA was employed to confirm the significant difference in each graph. n=2, *P<0.01.

glial fibrillary acidic protein (GFAP) was assessed in U-251MG P1 and U-251MGSC1 cells (**Figure 3B**) (see "Supplementary Figure 1" for full-length blot images). As the result, GFAP was clearly confirmed only in U-251MG cells but not in U-251MGSC1 cells implying U-251MGSC1 cells were undifferentiated.

Enhanced sphere forming ability and hyaluronan dependence of U-251MGSC1 cells

U-251MGSC1 cells were assessed for the sphere forming ability by limiting dilution method (**Figure 4**). When compared with U-251MG cells, U-251MGSC1 cells exhibited significantly higher sphere-forming ability.

We assessed the effect of hyaluronan on the proliferation of U-251MGSC1 cells. The number of U-251MGSC1 cells significantly increased in the presence of hyaluronic acid after 5 days (**Figure 5A**). On the other hand, hyaluronan did not affect on the proliferation of U-251MG cells. We also assessed the effect of hyaluronan on the ability of sphere formation. In the presence of hyaluronic acid, the sphere-forming ability of U-251MGSC1 cells was significantly enhanced in the range of 1.3 cells/well to 5 cells/well (**Figure 5B**).

Differentiation potential and tumorigenicity in vivo of U-251MGSC1 cells

From the results of GFAP expression (**Figure 3B**), U-251MG cells exhibited the differentiation which implied the cells secreted some factor inducing autocrine differentiation. Therefore, the conditioned medium (CM) of U-251MG cells were used to evaluate the differentiation potential of U-251MGSC1 cells. Since we did not know which concentration of condition medium was appropriate for inducing differentiation potential, we first confirmed differentiation potential with 10% and 50% CM of

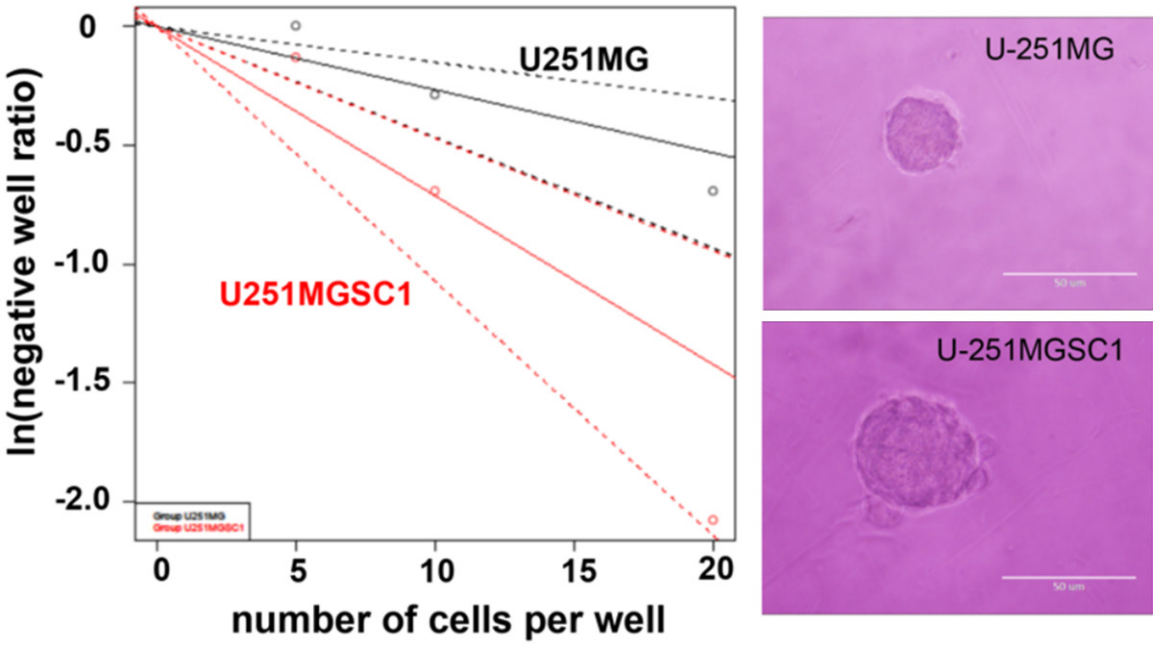

Figure 4. Sphere forming ability of U251MGSC1 cells compared to U251MG cells. Limiting dilution analysis was performed to evaluate the ability. The number of wells without spheres was counted where cells were seeded in 16 wells of 96-well plates. The number of the cells seeded in each 16-well was 20, 10, 5, and 2.5 cells/well, respectively. Each natural logarithm of "negative well number"/16 were plotted as "ln (negative well ratio)" for total number of cells. The trend line represents the estimated active cell frequency. The dotted lines give the 95% confidence interval. Typical spheres observed for U-251MG and U-251MGSC1 cells are shown on the right. A value obtained by dividing confidence intervals for 1 by the stem cell frequency indicates that the smaller the value, the higher the sphere formation ability.

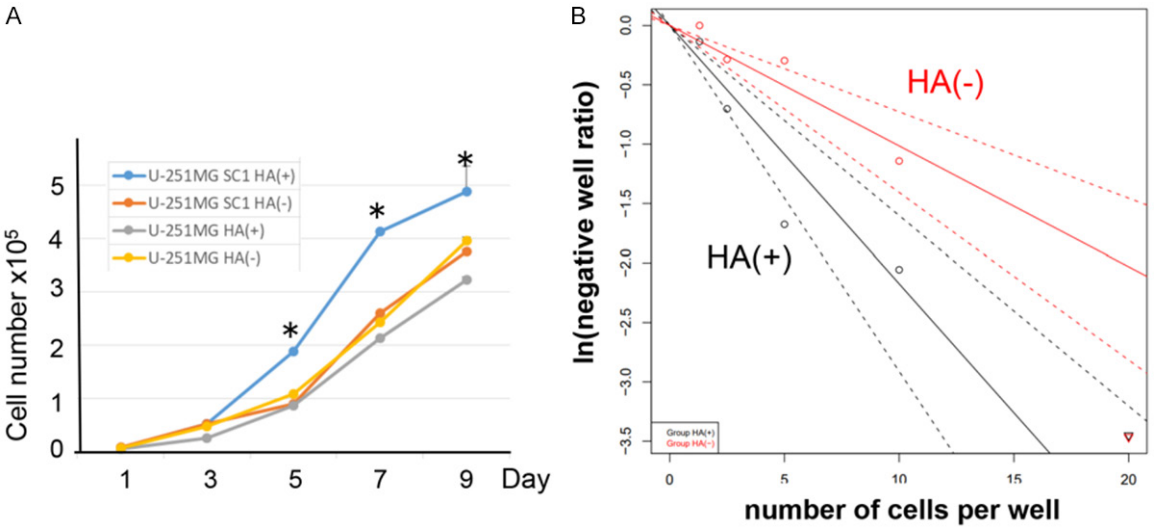

Figure 5. Hyaluronan-dependency in proliferation and self-renewal of U-251MGSC1 cell. A. Proliferation of U-251MG and U-251MGSC1 cells was compared in the presence or absence of hyaluronan. Significant differences were evaluated by ANOVA. *P<0.05. B. Sphere formation of U-251MGSC1 cells in the presence or absence of hyaluronan was assessed by limiting dilution analysis. The number of wells without spheres was counted where cells were seeded in 16 wells of 96-well plates. The number of the cells seeded in each 16-well was 20, 10, 5, 2.5 and 1.3 cells/well, respectively. Each natural logarithm of "negative well number"/16 were plotted as "ln (negative well ratio)" for total number of cells. The trend line represents the estimated active cell frequency. The dotted lines give the 95% confidence interval.

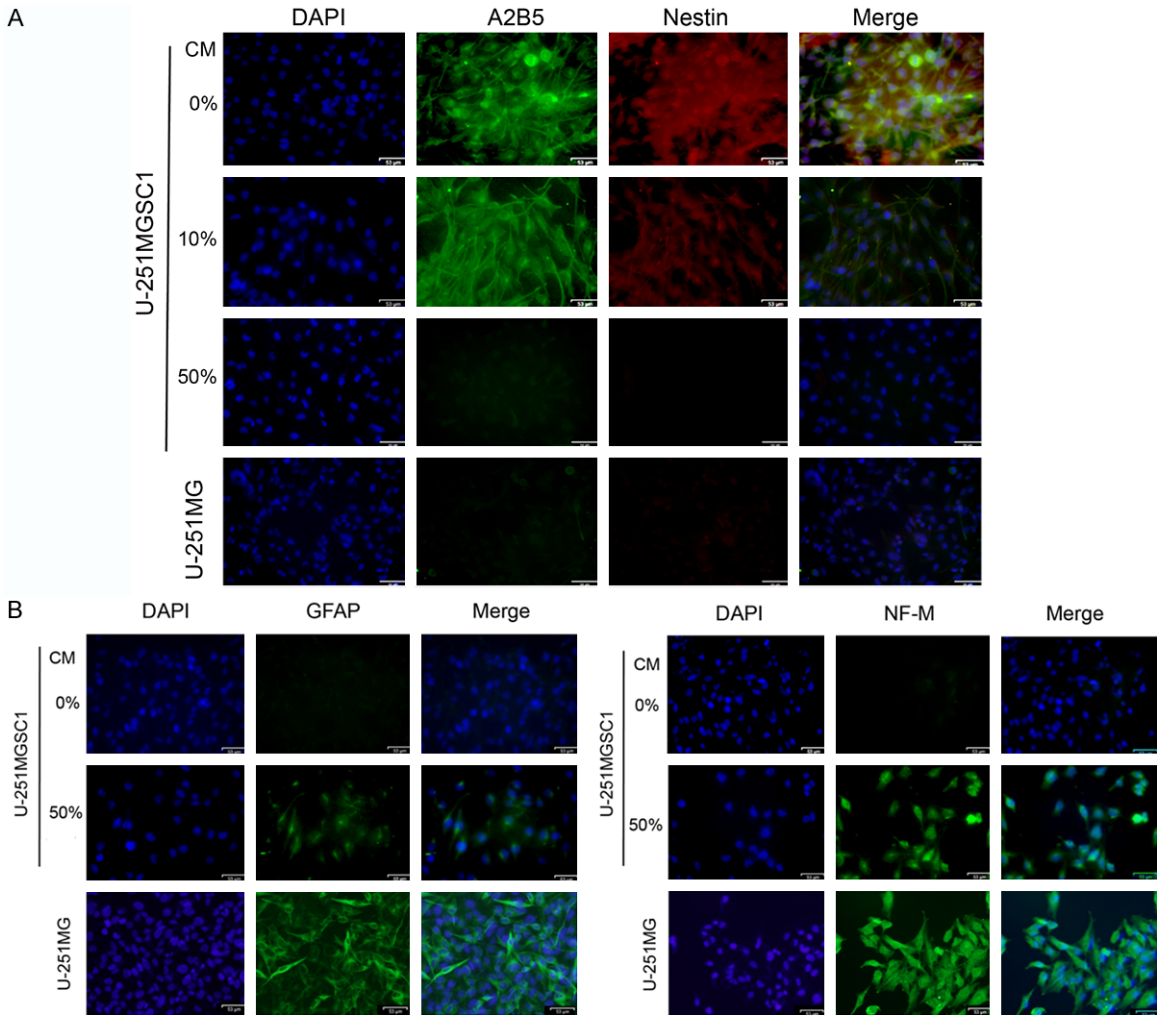

Figure 6. Differentiation of U-251MGSC1 cells in the presence of the condition medium from U-251MG cells. Immunofuluorescent cytochemistry of U-251MGSC1 cells against neural stem cell markers, A2B5 and Nestin (A) and neural cell markers, GFAP and NF-M (B) after exposed to 10% and 50% of CM for 2 weeks. 50% CM decreased the neural stem cell markers and enhance the neural cell markers suggesting the differentiation. Scale bar =53 μm.

U-251MG cells. As the results, treatment with 50% CM suppressed the expression of A2B5, a ganglioside marker for stem cells [24, 25] and Nestin, an intermediate filament protein expressed in stem cells of the central nervous system [23], down to the level in U-251MG cells while 10% CM did not (**Figure 6A**). Simultaneously, the expression of GFAP and neurofilament middle (NF-M), a marker of cytoskeleton in differentiated and mature neurons [26], in U-251MGSC1 cells were found to be enhanced. Nestin and NF-M are the components of intermediate filaments, which consist of six classes of proteins, as markers of nerve cells, unlike microtubules and actin fibers ubiquitously expressed in cells. As the results, the 50% CM enhanced the differentiation of U-251MGSC1 cells to the level as equivalent as that of U-251MG cells indicating the differentiation potential of U-251MGSC1 cells (**Figure 6B**).

To assess the tumorigenicity of U-251MGSC1 cells, 2×10^6 cells were subcutaneously transplanted into a nude mouse. After transplantation, the size of tumor measured up to 8 weeks (**Figure 7**). The tumors of both U-251MG and U-251MGSC1 cells started to grow after the third week. The growth rate of tumor from U-251MGSC1 cells was significantly higher than that of tumors made from U-251MG cells.

Immunohistochemistry of the sections from the tumors formed in nude mice exhibited the immunoreactive CD44 and SOX2 in

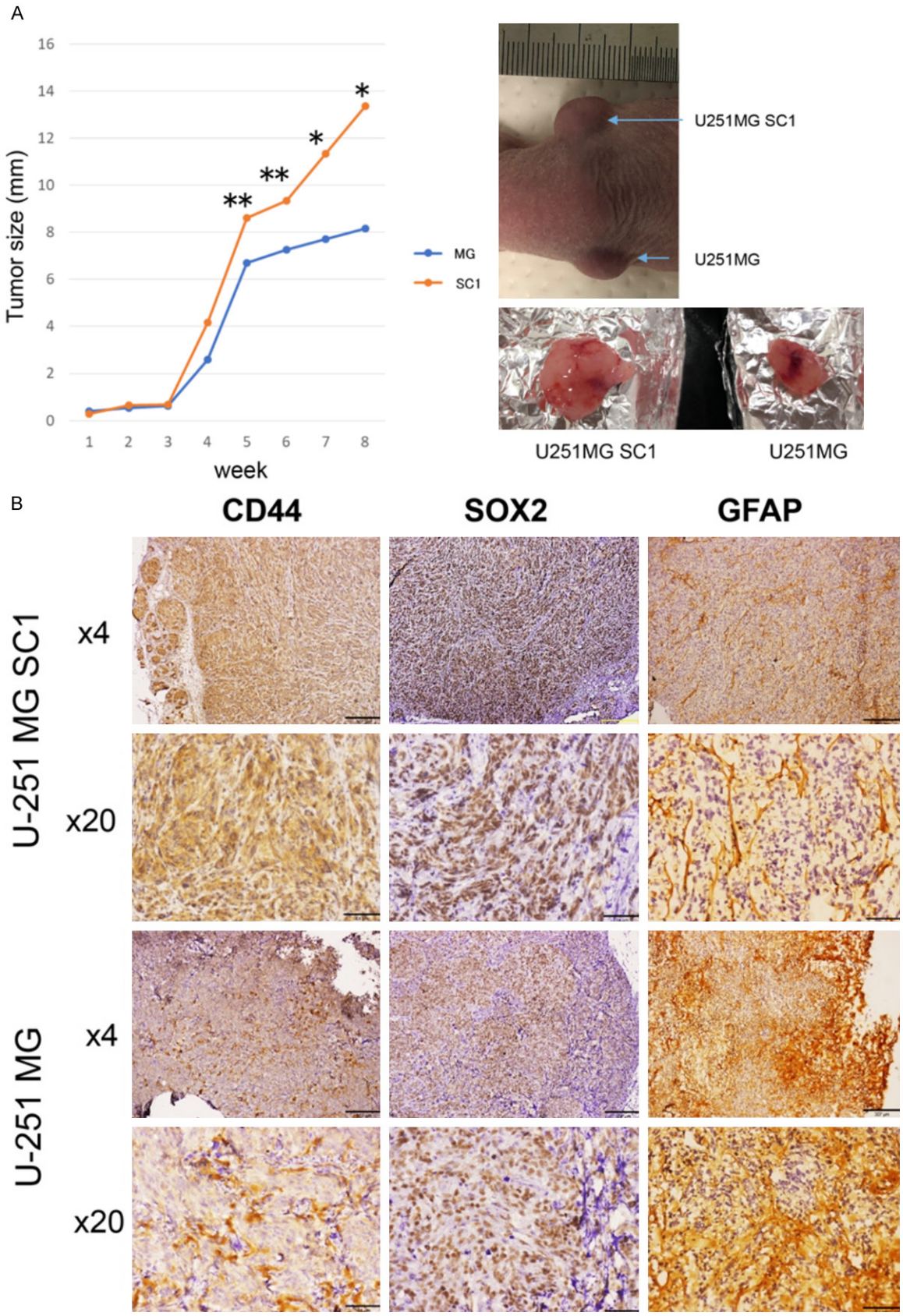
A
Tumor size (mm)
week
MG
SC1
U251MG SC1
U251MG
U251MG SC1
U251MG
B
CD44
SOX2
GFAP
U-251 MG SC1
x4
x20
U-251 MG
x4
x20

Figure 7. Tumorigenic potential of U-251MGSC1 cells. A. U-251MG cells and U-251MGSC1 cells were subcutaneously transplanted and the growth of tumor was monitored by the size from week 1 to week 8 after the cells were injected into nude mice. The tumor size was the average of the vertical and horizontal diameters. n=8. Significance was evaluated by t-test. *, P<0.05; **, P<0.01. Typical tumors in vivo and excised were shown on the right. B. Immunohistochemical analyses of the tumors. Paraffin embedded tissue sections were stained for anti-human CD44 antibody and anti-human SOX2. Frozen sections were analyzed for anti-human GFAP antibody. Maginifications of objective lens were × 4 and × 20.

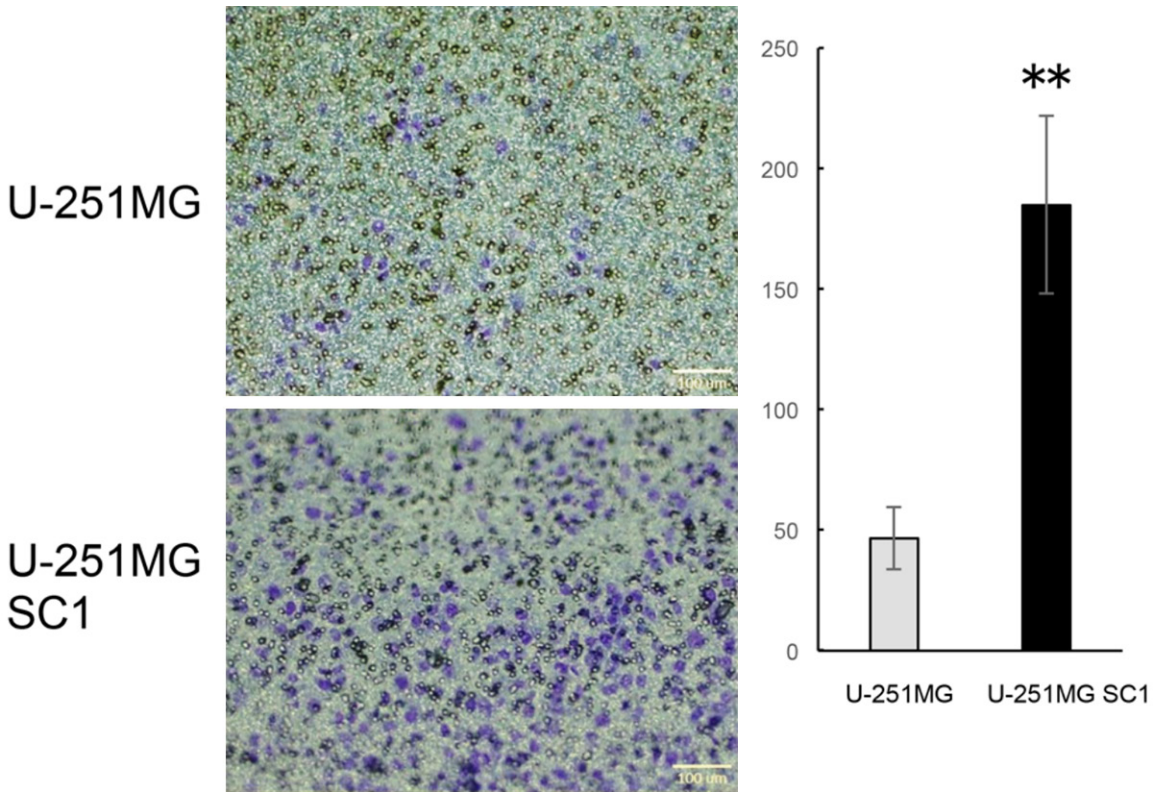

Figure 8. Metastatic potential of U-251MGSC1 cells. U-251MG cells and U-251MGSC1 cells in serum-free medium were seeded in a transmembrane-well and then the number of cells transferred to the serum containing medium were counted after 48 hr. n=3. Significance was evaluated by t-test. **, P<0.01. Maginifications of objective lens was × 4.

U-251MGSC1 cell derived tumor higher than those in U-251MG cell derived tumor. On the other hand, immunoreactive GFAP was found higher in U-251MG cell derived tumor than in U-251MGSC1 cell derived tumor.

Metastatic potential of the cells

In the process of cancer metastasis, cancer cell migration and infiltration are extremely important processes. Many researchers have studied that CSCs take an important role in producing cancer metastasis [44, 45]. We investigated the metastatic potential of U-251MGSC1 cells and performed transmembrane assay (**Figure 8**). The number of migrated cells of U-251MG cells was 46.6 whereas that of U-251MGSC1 was 184.8. This result shows that U-251MGSC1 cells have four times higher migration ability than the parental cells. Thus U-251MGSC1 cells were shown to be highly metastatic among the cells compared.

Discussion

Previously, we described the population of U-251MG P1 cells as the highly condensed population with the expression of CD44 and stemness markers when they were cultured as spheres in the presence of hyaluronic acid. CD44 is an adhesion molecule that binds to extracellular matrix, including hyaluronan, and

is used as an important marker in many cancer stem cell studies [46-48].

In this paper, we isolated five clones from U-251MG cells that grew in hyaluronan dependent manner. As was shown in cancer derived cell lines, heterogeneous population is observed within the cell line U251MG cells. The isolated five clones demonstrated different expression levels of stemness markers suggesting the heterogeneity (**Figure 1**). Among them U-251MGSC1 cells showed the highest expression of stemness markers implying the highest possibility as the stem-like cells. Therefore, we further characterized U-251MGSC1 cells as the candidate of CSCs. And U-251MGSC1 cells exhibited the highest expression stem cell genes when compared with the original parental cell lines U-251MG and U-251MG P1 (**Figure 2**).

SOX2 is known as one of the transcription factors, functioning to maintain stemness in human embryonic stem cells (hES cells), trophoblast stem cells (TS cells), and neural stem cells. SOX2 is also known as a glioma stem cell marker [49]. Nestin has been reported as a class VI intermediate filament protein expressed in stem cells of the central nervous system (CNS) [50]. And Nestin is not expressed in mature CNS. Therefore, Nestin is used as a marker in neural cells derived from hES cells and induced pluripotent stem cells. The highest expression of SOX2, Nestin, c-MYC, OCT3/4 and Nanog was recognized in U-251MGSC1 cells. Regarding KLF4 gene expression, U-251MG P1 showed the highest value, but only U-251MGSC1 cells showed high expression in all of these four stem cell markers. This indicates that U-251MGSC1 has strong character of stem cells. The expression levels of CD44 and CD133 confirmed by flow cytometry were further conceivable to conclude the stemness of U-251MGSC1 cells.

Gliomas are brain tumors that develop from glial cells found in the brain and spinal cord. GFAP is one of intermediate filament proteins and is specifically expressed in cells of the astroglial (astrocytic) lineage. Therefore, GFAP is widely used as an astrocyte marker in the brain, and glioma shows positive GFAP immunostaining [51, 52]. We confirmed the expression of GFAP by Western blotting in U-251MG cells (**Figure 3B**). Interestingly, the neuronal phenotype differentiation was induced in U-251MGSC1 cells when treated with 50% CM of U-251MG cells (**Figure 6A**, **6B**). This result indicates the differentiated phenotype of U-251MG cells secrete some differentiation factors. Taking these into consideration, we concluded that U-251MGSC1 cells had the potential of differentiation reside in cancer stem cells. Hyaluronan enhanced both proliferation and sphere formation of U-251MGSC1 cells indicating the significance of CD44 overexpression (**Figure 5**). Hyaluronic acid contributes to the maintenance and proliferation of stem cells when CD44 is overexpressed.

The limiting dilution method was employed to assess the ability to form spheres in U-251MG and U-251MGSC1 cells since sphere formation is considered to demonstrate self-renewal capacity [53-55]. As the result, U-251MGSC1 cells was shown to have self-renewal potential as a property of cancer stem cell (**Figure 4**). From the results of sphere formation assay, we expected high tumorigenic potential in U-251MGSC1 cells. When injected into mice, U-251MGSC1 cells showed significant tumorigenicity distinguished from that of U-251MG cells of which tumor growth appeared very slow and stopped.

From these tumors, expression of several genes was evaluated in the sections. Since the growth of U-251MGSC1 cell is dependent on hyaluronic acid, the expression of CD44 in the tumor was found overexpressed (**Figure 7B**). The expression of SOX2 was simultaneously found in the section of U-251MGSC1 tumor. These results are consistent with the results of gene expression in vitro (**Figure 2**). On the other hand, GFAP in U-251MGSC1 tumor was low. This result also agrees with the result in vitro (**Figure 3B**). These results indicate the tumor composed of undifferentiated cells may exhibit rapid growth and big size in a short period.

We confirmed the metastatic ability of U-251MGSC1 cells, which is consistent with the high metastatic potential of CSCs. Additionally, many studies have shown that stem cell markers such as SOX2, Olig2, and Nestin are also involved in cancer metastasis [38, 56, 57]. The high metastatic potential of U-251MGSC1 could be elucidated by the expression of these markers although more detailed study, such as metastasis in vivo, is required. We are further

investigating the characters of U-251MGSC1 cells defining as CSCs.

Conclusions

In this paper, five different clonal cells were isolated from human glioma derived U-251MG cells, which consist of heterogeneous population of cells, showing different gene expression. One of these clones, U-251MGSC1 cell, was successfully characterized as CSCs by the high expression of stem cell markers, metastasis ability, the sphere forming and differentiation ability as well as tumorigenicity in vivo. The growth of U-251MGSC1 cells was dependent of hyaluronan due to the overexpression of CD44. U-251MGSC1 cells will be a good tool to develop effective therapeutic agents against CSCs and to elucidate the properties of glioma derived CSCs and the mechanism of tumor development in brain.

We are further aiming at the establishment of CSC lines derived from various cancers such as in pancreas, breast, lung and etc. in the future.

Acknowledgements

The authors acknowledge Mr. Rin Ito and Ms. Hagar A Abu Quora for their helpful assistance. This study was partly funded by ABioTech, Co., Ltd (Seoul, Korea).

Disclosure of conflict of interest

None.

Address correspondence to: Masaharu Seno, Laboratory of Nano-Biotechnology, Graduate School of Interdisciplinary Science and Engineering in Health Systems, Okayama University, Okayama 700-8530, Japan. E-mail: mseno@okayama-u.ac.jp

References

[1] Dagenais GR, Leong DP, Rangarajan S, Lanas F, Lopez-Jaramillo P, Gupta R, Diaz R, Avezum A, Oliveira GB and Wielgosz A. Variations in common diseases, hospital admissions, and deaths in middle-aged adults in 21 countries from five continents (PURE): a prospective cohort study. Lancet 2020; 395: 785-794.

[2] Vlashi E and Pajonk F. Cancer stem cells, cancer cell plasticity and radiation therapy. Semin Cancer Biol 2015; 31: 28-35.

[3] Chu DT, Nguyen TT, Tien NLB, Tran DK, Jeong JH, Anh PG, Thanh VV, Truong DT and Dinh TC. Recent progress of stem cell therapy in cancer treatment: molecular mechanisms and potential applications. Cells 2020; 9: 563.

[4] Nimmakayala RK, Batra SK and Ponnusamy MP. Unraveling the journey of cancer stem cells from origin to metastasis. Biochim Biophys Acta Rev Cancer 2019; 1871: 50-63.

[5] Dick JE. Stem cell concepts renew cancer research. Blood 2008; 112: 4793-4807.

[6] S Franco S, Szczesna K, Iliou MS, Al-Qahtani M, Mobasheri A, Kobolák J and Dinnyés A. In vitro models of cancer stem cells and clinical applications. BMC Cancer 2016; 16 Suppl 2: 738.

[7] Iqbal W, Alkarim S, AlHejin A, Mukhtar H and Saini KS. Targeting signal transduction pathways of cancer stem cells for therapeutic opportunities of metastasis. Oncotarget 2016; 7: 76337.

[8] Oliphant MUJ, Vincent MY, Galbraith MD, Pandey A, Zaberezhnyy V, Rudra P, Johnson KR, Costello JC, Ghosh D, DeGregori J, Espinosa JM and Ford HL. SIX2 mediates late-stage metastasis via direct regulation of SOX2 and induction of a cancer stem cell program. Cancer Res 2019; 79: 720-734.

[9] Mavilio F, Simeone A, Boncinelli E and Andrews PW. Activation of four homeobox gene clusters in human embryonal carcinoma cells induced to differentiate by retinoic acid. Differentiation 1988; 37: 73-79.

[10] Andrews PW. Human teratocarcinomas. Biochim Biophys Acta 1988; 948: 17-36.

[11] Fenderson BA, Andrews PW, Nudelman E, Clausen H and Hakomori S. Glycolipid core structure switching from globo- to lacto- and ganglio-series during retinoic acid-induced differentiation of TERA-2-derived human embryonal carcinoma cells. Dev Biol 1987; 122: 21-34.

[12] Andrews PW, Damjanov I, Simon D, Banting GS, Carlin C, Dracopoli NC and Føgh J. Pluripotent embryonal carcinoma clones derived from the human teratocarcinoma cell line Tera-2. Differentiation in vivo and in vitro. Lab Invest 1984; 50: 147-162.

[13] Soule HD, Maloney TM, Wolman SR, Peterson WD Jr, Brenz R, McGrath CM, Russo J, Pauley RJ, Jones RF and Brooks SC. Isolation and characterization of a spontaneously immortalized human breast epithelial cell line, MCF-10. Cancer Res 1990; 50: 6075-6086.

[14] Seystahl K, Wick W and Weller M. Therapeutic options in recurrent glioblastoma–an update. Crit Rev Oncol Hematol 2016; 99: 389-408.

[15] Ricard D, Idbaih A, Ducray F, Lahutte M, Hoang-Xuan K and Delattre JY. Primary brain tumours in adults. Lancet 2012; 379: 1984-1996.

[16] Sugli Y, Kasai T, Ikeda M, Vaidyanath A, Kumon K, Mizutani A, Seno A, Tokutaka H, Kudoh T and Seno M. A unique procedure to identify

cell surface markers through a spherical self-organizing map applied to DNA microarray analysis. Biomark Cancer 2016; 8: 17-23.
[17] Jadus MR, Chen Y, Boldaji MT, Delgado C, Sanchez R, Douglass T, Al-Atar U, Schulz W, Lloyd C and Wepsic HT. Human U251MG glioma cells expressing the membrane form of macrophage colony-stimulating factor (mM-CSF) are killed by human monocytes in vitro and are rejected within immunodeficient mice via paraptosis that is associated with increased expression of three different heat shock proteins. Cancer Gene Ther 2003; 10: 411-420.
[18] Ogino A, Sano E, Ochiai Y, Yamamuro S, Tashiro S, Yachi K, Ohta T, Fukushima T, Okamoto Y, Tsumoto K, Ueda T, Yoshino A and Katayama Y. Efficacy of ribavirin against malignant glioma cell lines. Oncol Lett 2014; 8: 2469-2474.
[19] Chanmee T, Ontong P, Mochizuki N, Kongtawelert P, Konno K and Itano N. Excessive hyaluronan production promotes acquisition of cancer stem cell signatures through the coordinated regulation of Twist and the transforming growth factor beta (TGF-beta)-Snail signaling axis. J Biol Chem 2014; 289: 26038-26056.
[20] Vaidyanath A, Mahmud HB, Khayrani AC, KoKo Oo A, Seno A, Asakura M, Kasai T and Seno M. Hyaluronic acid mediated enrichment of CD44 expressing glioblastoma stem cells in U251MG xenograft mouse model. Journal of Stem Cell Research & Therapy 2017; 07.
[21] Hu Y and Smyth GK. ELDA: extreme limiting dilution analysis for comparing depleted and enriched populations in stem cell and other assays. J Immunol Methods 2009; 347: 70-78.
[22] Taswell C. Limiting dilution assays for the determination of immunocompetent cell frequencies. I. Data analysis. J Immunol 1981; 126: 1614-1619.
[23] Flecknell P. Laboratory animal anaesthesia. Academic Press 2015.
[24] Blum D and LaBarge S; Reproducibility Project: Cancer Biology. Registered report: tumour micro-environment elicits innate resistance to RAF inhibitors through HGF secretion. Elife 2014; 3: e04034.
[25] Li L and Hanahan D. Hijacking the neuronal NMDAR signaling circuit to promote tumor growth and invasion. Cell 2013; 153: 86-100.
[26] Schatton T, Frank NY and Frank MH. Identification and targeting of cancer stem cells. Bioessays 2009; 31: 1038-1049.
[27] Mahmud H, Kasai T, Khayrani AC, Asakura M, Oo AKK, Du J, Vaidyanath A, El-Ghlban S, Mizutani A, Seno A, Murakami H, Masuda J and Seno M. Targeting glioblastoma cells expressing CD44 with liposomes encapsulating doxorubicin and displaying chlorotoxin-IgG Fc fusion protein. Int J Mol Sci 2018; 19: 659.
[28] Modrek AS, Golub D, Khan T, Bready D, Prado J, Bowman C, Deng J, Zhang G, Rocha PP, Raviram R, Lazaris C, Stafford JM, LeRoy G, Kader M, Dhaliwal J, Bayin NS, Frenster JD, Serrano J, Chiriboga L, Baitalmal R, Nanjangud G, Chi AS, Golfinos JG, Wang J, Karajannis MA, Bonneau RA, Reinberg D, Tsirigos A, Zagzag D, Snuderl M, Skok JA, Neubert TA and Placantonakis DG. Low-grade astrocytoma mutations in IDH1, P53, and ATRX cooperate to block differentiation of human neural stem cells via repression of SOX2. Cell Rep 2017; 21: 1267-1280.
[29] Berezovsky AD, Poisson LM, Cherba D, Webb CP, Transou AD, Lemke NW, Hong X, Hasselbach LA, Irtenkauf SM, Mikkelsen T and deCarvalho AC. Sox2 promotes malignancy in glioblastoma by regulating plasticity and astrocytic differentiation. Neoplasia 2014; 16: 193-206, 206 e119-125.
[30] Ikushima H, Todo T, Ino Y, Takahashi M, Saito N, Miyazawa K and Miyazono K. Glioma-initiating cells retain their tumorigenicity through integration of the Sox axis and Oct4 protein. J Biol Chem 2011; 286: 41434-41441.
[31] Karmakar S, Seshacharyulu P, Lakshmanan I, Vaz AP, Chugh S, Sheinin YM, Mahapatra S, Batra SK and Ponnusamy MP. hPaf1/PD2 interacts with OCT3/4 to promote self-renewal of ovarian cancer stem cells. Oncotarget 2017; 8: 14806.
[32] Niu CS, Li DX, Liu YH, Fu XM, Tang SF and Li J. Expression of NANOG in human gliomas and its relationship with undifferentiated glioma cells. Oncol Rep 2011; 26: 593-601.
[33] Habu N, Imanishi Y, Kameyama K, Shimoda M, Tokumaru Y, Sakamoto K, Fujii R, Shigetomi S, Otsuka K, Sato Y, Watanabe Y, Ozawa H, Tomita T, Fujii M and Ogawa K. Expression of Oct3/4 and Nanog in the head and neck squamous carcinoma cells and its clinical implications for delayed neck metastasis in stage I/II oral tongue squamous cell carcinoma. BMC Cancer 2015; 15: 730.
[34] Friedmann-Morvinski D and Verma IM. Dedifferentiation and reprogramming: origins of cancer stem cells. EMBO Rep 2014; 15: 244-253.
[35] Cheng L, Huang Z, Zhou W, Wu Q, Donnola S, Liu JK, Fang X, Sloan AE, Mao Y, Lathia JD, Min W, McLendon RE, Rich JN and Bao S. Glioblastoma stem cells generate vascular pericytes to support vessel function and tumor growth. Cell 2013; 153: 139-152.
[36] Wang J, Wang H, Li Z, Wu Q, Lathia JD, McLendon RE, Hjelmeland AB and Rich JN. c-Myc is required for maintenance of glioma can-

cer stem cells. PLoS One 2008; 3: e3769-e3769.
[37] Patel AP, Tirosh I, Trombetta JJ, Shalek AK, Gillespie SM, Wakimoto H, Cahill DP, Nahed BV, Curry WT, Martuza RL, Louis DN, Rozenblatt-Rosen O, Suvà ML, Regev A and Bernstein BE. Single-cell RNA-seq highlights intratumoral heterogeneity in primary glioblastoma. Science 2014; 344: 1396-1401.
[38] Ligon KL, Huillard E, Mehta S, Kesari S, Liu H, Alberta JA, Bachoo RM, Kane M, Louis DN, DePinho RA, Anderson DJ, Stiles CD and Rowitch DH. Olig2-regulated lineage-restricted pathway controls replication competence in neural stem cells and malignant glioma. Neuron 2007; 53: 503-517.
[39] Ghaleb AM and Yang VW. Kruppel-like factor 4 (KLF4): what we currently know. Gene 2017; 611: 27-37.
[40] Ma J, Yao Y, Wang P, Liu Y, Zhao L, Li Z, Li Z and Xue Y. MiR-152 functions as a tumor suppressor in glioblastoma stem cells by targeting Krüppel-like factor 4. Cancer Lett 2014; 355: 85-95.
[41] Schuettpelz LG, Gopalan PK, Giuste FO, Romine MP, van Os R and Link DC. Kruppel-like factor 7 overexpression suppresses hematopoietic stem and progenitor cell function. Blood 2012; 120: 2981-2989.
[42] Bexell D, Gunnarsson S, Siesjö P, Bengzon J and Darabi A. CD133+ and nestin+ tumor-initiating cells dominate in N29 and N32 experimental gliomas. Int J Cancer 2009; 125: 15-22.
[43] Glumac PM and LeBeau AM. The role of CD133 in cancer: a concise review. Clin Transl Med 2018; 7: 18.
[44] Shiozawa Y, Nie B, Pienta KJ, Morgan TM and Taichman RS. Cancer stem cells and their role in metastasis. Pharmacol Ther 2013; 138: 285-293.
[45] Afify SM, Hassan G, Osman A, Calle AS, Nawara HM, Zahra MH, El-Ghlban S, Mansour H, Alam MJ, Abu Quora HA, Du J, Seno A, Iwasaki Y and Seno M. Metastasis of cancer stem cells developed in the microenvironment of hepatocellular carcinoma. Bioengineering (Basel) 2019; 6: 73.
[46] Li C, Heidt DG, Dalerba P, Burant CF, Zhang L, Adsay V, Wicha M, Clarke MF and Simeone DM. Identification of pancreatic cancer stem cells. Cancer Res 2007; 67: 1030-1037.
[47] Tomao F, Papa A, Strudel M, Rossi L, Lo Russo G, Benedetti Panici P, Ciabatta FR and Tomao S. Investigating molecular profiles of ovarian cancer: an update on cancer stem cells. J Cancer 2014; 5: 301-310.
[48] Bourguignon LY, Shiina M and Li JJ. Hyaluronan-CD44 interaction promotes oncogenic signaling, microRNA functions, chemoresistance, and radiation resistance in cancer stem cells leading to tumor progression. Adv Cancer Res 2014; 123: 255-275.
[49] Hemmati HD, Nakano I, Lazareff JA, Masterman-Smith M, Geschwind DH, Bronner-Fraser M and Kornblum HI. Cancerous stem cells can arise from pediatric brain tumors. Proc Natl Acad Sci U S A 2003; 100: 15178-15183.
[50] Bernal A and Arranz L. Nestin-expressing progenitor cells: function, identity and therapeutic implications. Cell Mol Life Sci 2018; 75: 2177-2195.
[51] van Bodegraven EJ, van Asperen JV, Robe PAJ and Hol EM. Importance of GFAP isoform-specific analyses in astrocytoma. Glia 2019; 67: 1417-1433.
[52] Battaglia RA, Beltran AS, Delic S, Dumitru R, Robinson JA, Kabiraj P, Herring LE, Madden VJ, Ravinder N, Willems E, Newman RA, Quinlan RA, Goldman JE, Perng MD, Inagaki M and Snider NT. Site-specific phosphorylation and caspase cleavage of GFAP are new markers of Alexander disease severity. Elife 2019; 8: e47789.
[53] Bahmad HF, Cheaito K, Chalhoub RM, Hadadeh O, Monzer A, Ballout F, El-Hajj A, Mukherji D, Liu YN, Daoud G and Abou-Kheir W. Sphere-formation assay: three-dimensional in vitro culturing of prostate cancer stem/progenitor sphere-forming cells. Front Oncol 2018; 8: 347.
[54] Basuroy U, Basilico C and Mansukhani A. Sphere formation (osteosphere/sarcopshere) assay. BIO-PROTOCOL 2012.
[55] Bono B, Ostano P, Peritore M, Gregnanin I, Belgiovine C, Liguori M, Allavena P, Chiorino G, Chiodi I and Mondello C. Cells with stemness features are generated from in vitro transformed human fibroblasts. Sci Rep 2018; 8: 13838.
[56] Chaudhary S, Islam Z, Mishra V, Rawat S, Ashraf GM and Kolatkar PR. Sox2: a regulatory factor in tumorigenesis and metastasis. Curr Protein Pept Sci 2019; 20: 495-504.
[57] Matsuda Y, Yoshimura H, Ueda J, Naito Z, Korc M and Ishiwata T. Nestin delineates pancreatic cancer stem cells in metastatic foci of NOD/Shi-scid IL2Rγnull (NOG) mice. Am J Pathol 2014; 184: 674-685.
[58] Zhu L and Chen L. Progress in research on paclitaxel and tumor immunotherapy. Cell Mol Biol Lett 2019; 24: 40.
[59] Dasari S and Tchounwou PB. Cisplatin in cancer therapy: molecular mechanisms of action. Eur J Pharmacol 2014; 740: 364-378.
[60] Tacar O, Sriamornsak P and Dass CR. Doxorubicin: an update on anticancer molecular

action, toxicity and novel drug delivery systems. J Pharm Pharmacol 2013; 65: 157-170.
[61] Desai A, Yan Y and Gerson SL. Concise reviews: cancer stem cell targeted therapies: toward clinical success. Stem Cells Transl Med 2019; 8: 75-81.
[62] Hellmann MD, Paz-Ares L, Bernabe Caro R, Zurawski B, Kim SW, Carcereny Costa E, Park K, Alexandru A, Lupinacci L, de la Mora Jimenez E, Sakai H, Albert I, Vergnenegre A, Peters S, Syrigos K, Barlesi F, Reck M, Borghaei H, Brahmer JR, O'Byrne KJ, Geese WJ, Bhagavatheeswaran P, Rabindran SK, Kasinathan RS, Nathan FE and Ramalingam SS. Nivolumab plus ipilimumab in advanced non-small-cell lung cancer. N Engl J Med 2019; 381: 2020-2031.
[63] Hosomi Y, Morita S, Sugawara S, Kato T, Fukuhara T, Gemma A, Takahashi K, Fujita Y, Harada T, Minato K, Takamura K, Hagiwara K, Kobayashi K, Nukiwa T and Inoue A. Gefitinib alone versus gefitinib plus chemotherapy for non-small-cell lung cancer with mutated epidermal growth factor receptor: NEJ009 study. J Clin Oncol 2020; 38: 115-123.
[64] Abdollahpour-Alitappeh M, Lotfinia M, Bagheri N, Sineh Sepehr K, Habibi-Anbouhi M, Kobarfard F, Balalaie S, Foroumadi A, Abbaszadeh-Goudarzi G, Abbaszadeh-Goudarzi K and Abolhassani M. Trastuzumab-monomethyl auristatin E conjugate exhibits potent cytotoxic activity in vitro against HER2-positive human breast cancer. J Cell Physiol 2019; 234: 2693-2704.
[65] Deng C, Pan B and O'Connor OA. Brentuximab vedotin. Clin Cancer Res 2013; 19: 22-27.
[66] Amiri Darban S, Nikoofal-Sahlabadi S, Amiri N, Kiamanesh N, Mehrabian A, Zendehbad B, Gholizadeh Z and Jaafari MR. Targeting the leptin receptor: to evaluate therapeutic efficacy and anti-tumor effects of Doxil, in vitro and in vivo in mice bearing C26 colon carcinoma tumor. Colloids Surf B Biointerfaces 2018; 164: 107-115.
[67] Lamb YN and Scott LJ. Liposomal irinotecan: a review in metastatic pancreatic adenocarcinoma. Drugs 2017; 77: 785-792.

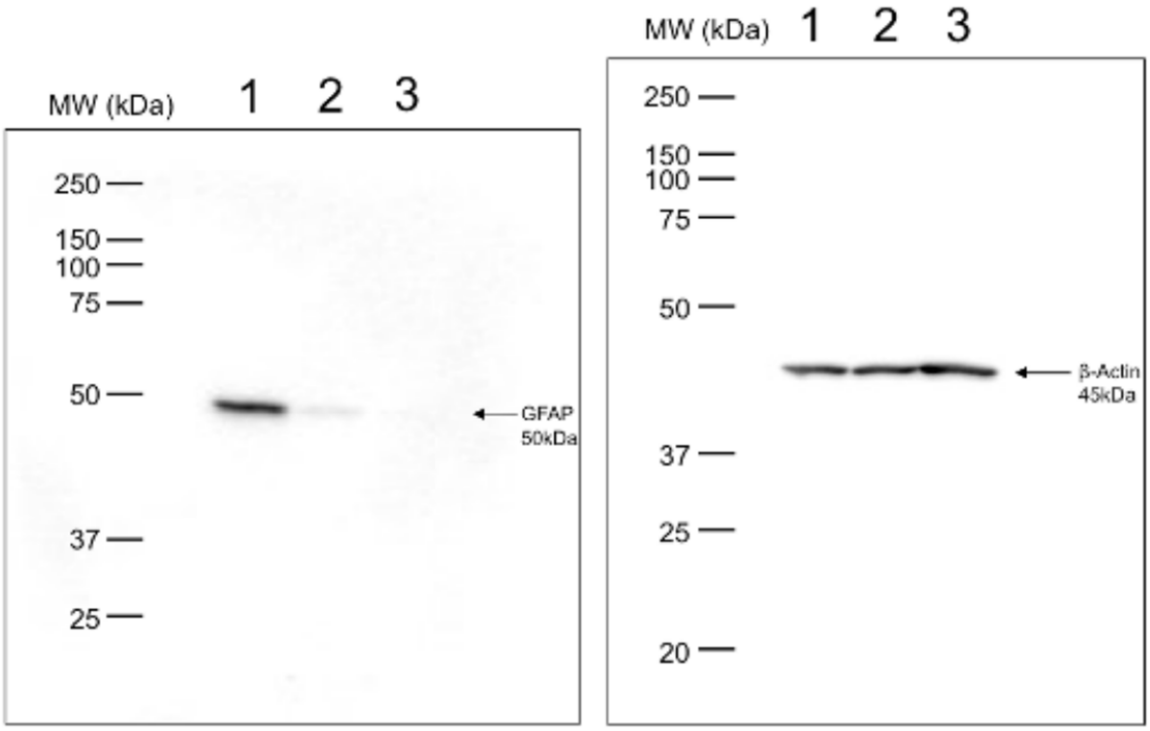

Supplementary Figure 1. Full-length blot images of **Figure 3B**. Western blotting result of GFAP. Anti-GFAP antibody (J0510, Santa Cruz Biotechnology, CA) diluted to 1/1000. Western blotting results of anti-β-actin. Anti-β-actin antibody (4970S, Cell Signaling, MA) diluted to 1/1000. Each lane shows extracts from U251MG cells (lane 1), U251MG P1 cells (lane 2), and U251MGSC1 cells (lane 3).